Folding Topologies of Human Interleukin-6 and Its Mutants As Studied by NMR Spectroscopy†

Chiaki Nishimura,*,‡ Ayako Watanabe,‡,|| Hiroaki Gouda,§ Ichio Shimada,‡ and Yoji Arata‡,⊥

Faculty of Pharmaceutical Sciences, University of Tokyo, Hongo, Bunkyo-ku, Tokyo 113, Japan, and Advanced Research Laboratory Hitachi, Ltd., Hatoyama, Saitama 350-03, Japan

Received August 17, 1995; Revised Manuscript Received October 18, 1995⊗

ABSTRACT: To understand the structure−function relationship in the human interleukin-6 (IL-6) system, comparative studies were performed on the basis of NMR data obtained using the wild-type IL-6 and six mutants. In each of the six mutants, either Leu152, Leu159, Leu166, Leu168, Leu175, or Leu182, which exist in the C-terminal receptor-binding region, was substituted with Val. The resonance assignments of Val, Ile, Leu, and Phe residues were made by using specific double-labeling and site-specific mutagenesis strategies. On the basis of chemical shift and NOE data collected for six IL-6 mutants and those for the wild-type IL-6, we analyzed the structural changes induced by the substitution of each of the six Leu residues. The NMR data showed that substitution of Leu182 with Val (L182V) induced no structural change in IL-6, suggesting that Leu182 is located on the surface of the IL-6 molecule. A significant decrease in receptor-binding activity was observed in the L182V mutant. It was concluded that the side chain of Leu182 is directly involved in receptor binding. Substitution of Leu175 with Val (L175V) was shown to induce a significant structural change in IL-6. The NMR data are discussed on the basis of the location of four helix elements and an up−up−down−down helix topology of the predicted structure of IL-6 [Bazan, J. F. (1991) *Neuron 7*, 197−208]. It is possible that helix D bent more sharply toward helix B in the L175V mutant than in the wild-type IL-6 to maintain a closely packed and solvent-inaccessible core formed in the mutated region. It is suggested that the kink of helix D is related to the decrease in receptor-binding activity in the L175V mutant. On the basis of the observed NOE network, the folding topology of IL-6 was analyzed. A comparison of the folding topology of IL-6 with that of human granulocyte colony-stimulating factor determined by X-ray crystallography [Hill, C. P., Osslund, T. D., & Eisenberg, D. (1993) *Proc. Natl. Acad. Sci. U.S.A. 90*, 5167−5171] indicated that IL-6 has a significant similarity of folding topology to that of human granulocyte colony-stimulating factor.

Interleukin-6 (IL-6)[1] is a multifunctional cytokine that modulates the growth and differentiation of various cells (Kishimoto & Hirano, 1988). IL-6 exerts function when it binds to the specific high-affinity receptor complex consisting of two different subunits, i.e., the gp80 binding subunit and the gp130 signal transducer subunit (Taga et al., 1989). The gp130 also functions as a signal transducer for oncostatin M, leukemia inhibiting factor (LIF), ciliary neurotrophic factor, and IL-11 (Kishimoto et al., 1992). It has been reported that the unusual increase in the expression of IL-6 is involved in various diseases. An IL-6 antagonist, which binds only the gp80 receptor but not the gp130 signal transducer, has therefore been sought (Savino et al., 1994a,b; Brakenhoff et al., 1994; Ehlers et al., 1995; Paonessa et al., 1995). The design of the antagonist obviously has to be based on data for the tertiary structure of IL-6.

Many hematopoietic and neuropoietic cytokines were predicted to share a common four-helical structure (Bazan, 1991). Sprang proposed, on the basis of structural comparison of the nine structure available helical cytokines, that cytokines can be divided into two divergent subgroups with either a short helix chain or a long helix chain (Sprang & Bazan, 1993). The long helix chain cytokine contains helices comprising about 25 amino acids, which are more tightly packed in structure than those that exist in the short chain group. Although NMR studies of human (Nishimura et al., 1990, 1991b; Proudfoot et al., 1993) and murine (Morton et al., 1995) IL-6's have been performed, the three-dimensional structure of IL-6 is not clear. Prediction of the secondary structure of IL-6 has been made on the basis of the known structures of other cytokines (Bazan, 1990, 1991; Sprang & Bazan, 1993). IL-6 has been classified into the group of the long helix chain cytokines, which includes growth hormone, granulocyte colony-stimulating factor (G-CSF), interferon-β, LIF, prolactin, IL-11, IL-12, erythropoietin, oncostatin M, and ciliary neurotrophic factor. Among long helix chain cytokines, the three-dimensional structures of human growth hormone (de Vos et al., 1992), human G-CSF (Hill et al., 1993), murine interferon-β (Senda et al., 1992),

† This study was supported in part by a Grant-in-Aid for Scientific Research from the Ministry of Education, Science and Culture of Japan and by grants from the Mochida Memorial Foundation for Medical and Pharmaceutical Research.

* Author to whom correspondence should be addressed.
‡ University of Tokyo.
§ Advanced Research Laboratory Hitachi, Ltd.
|| Present address: Institute of Biological Science, Mitsui Pharmaceuticals, Inc., Mobara, Chiba 297, Japan.
⊥ Present address: Water Research Institute, Sengen 2-1-6, Tsukuba, Ibaraki 305, Japan

⊗ Abstract published in *Advance ACS Abstracts,* December 15, 1995.

[1] Abbreviations: IL-6, interleukin-6; LIF, leukemia inhibiting factor; G-CSF, granulocyte colony-stimulating factor; WT, wild-type; *E. coli*, *Escherichia coli*; HPLC, high-performance liquid chromatography; NOESY, nuclear Overhauser effect spectroscopy; HOHAHA, homonuclear Hartmann−Hahn spectroscopy.

0006-2960/96/0435-273$12.00/0

and murine LIF (Robinson et al., 1994) have been determined by X-ray crystallography. On the basis of the X-ray structure of G-CSF, models of the three-dimensional structure of human IL-6 were built (Savino et al., 1994a; Ehlers et al., 1994).

In the C-terminal region of human IL-6, which is composed of 185 amino acid residues, there are two sets of three periodic Leu residues that appear every seven residues, i.e., Leu152, Leu159, and Leu166 and Leu168, Leu175, and Leu182. In previous studies, each of the Leu residues has been substituted by a Val residue (Nishimura et al., 1991a, 1992). This is because (1) six Leu residues are conserved in many cytokines, suggesting that they play an important role in maintaining the proper structure for the expression of biological functions, and (2) a conservative amino acid replacement of a Leu residue with a Val residue is known to influence the local conformation of the protein without disturbing the overall structure. The results of the site-directed mutagenesis have shown that the Leu residues, especially Leu168, Leu175, and Leu185, play an important role in gp80 receptor binding (Nishimura et al., 1992). Other site-directed mutagenesis studies of IL-6 have also shown that the amino acid residues in the C-terminal region play an important role in gp80 receptor binding (Krüttgen et al., 1990; Leebeek et al., 1992; Fontaine et al., 1994).

A number of studies have been reported so far concerning the structure−function relationships of IL-6. However, very little is known about the relationship between the receptor-binding activity and the tertiary structure. The aim of the present investigation is to discuss the role of the Leu residues that exist in the C-terminal receptor-binding region of IL-6. On the basis of chemical shift and NOE data collected for six IL-6 mutants and those for the wild-type (WT) IL-6, we will analyze the structural changes induced by the substitution of each of the six Leu residues. We will also discuss how the changes in the tertiary structure of the receptor-binding region affect the receptor-binding activity of IL-6.

MATERIALS AND METHODS

Materials. L-[^{15}N]Tyr was purchased from Isocommerz GmbH. [1-^{13}C]Cystine was a gift from Dr. N. Sugita. All other ^{13}C- and ^{15}N-labeled amino acids were purchased from ICON Services Inc. The isotope enrichment is 95% or greater for each of the amino acids. Thrombin was obtained from Mochida Pharmaceutical Co. All other chemicals were of reagent grade and used without further purification.

Protein Expression and Purification. The WT and all mutant IL-6's were expressed in *Escherichia coli* as a human growth hormone fusion protein, cleaved from the fusion protein by thrombin, and finally subjected to high-performance liquid chromatography (HPLC) purification by using an ion exchange column (Asagoe et al., 1988). The *E. coli* strain RB791 containing the plasmid encoding human IL-6 and growth hormone was cultured for 2 h at 37 °C in M9 minimum medium (1 L) containing 50 mg of stable-isotope-labeled amino acid(s) and the other nonlabeled amino acids without glucose. Indoleacrylic acid was added to the culture medium to a final concentration of 25 μg/mL, and the culture was continued at 37 °C for an additional 10 h. The cells were harvested by centrifugation, and the cell pellet was suspended in 50 mM Tris-HCl (pH 8.0) and disrupted by sonication. After centrifugation, inclusion bodies of IL-6−growth hormone fusion protein were recovered from the pellet fraction and dissolved in 50 mM Tris-HCl (pH 8.0) containing 6M guanidine hydrochloride and 10 mM dithiothreitol. The denatured protein solution was dialyzed against 2 M urea in 50 mM Tris-HCl (pH 8.0) in the presence of the glutathione redox system, followed by the dialysis against the same buffer containing 1 M urea. The resulting partially refolded fusion protein was cleaved by 800 units of thrombin into growth hormone and IL-6. After 18-h of incubation at 37 °C, the powder of guanidine hydrochloride and dithiothreitol was added directly to the protein solution to final concentrations of 6 M and 10 mM, respectively. The protein solution was dialyzed against 50 mM Tris-HCl (pH 8.0) containing 2 M and subsequently 1 M guanidine hydrochloride in the presence of the glutathione redox system. Finally, the protein solution was dialyzed against six changes of 5 mM Tris-HCl (pH 8.0) and subjected to HPLC purification. The protein solution was applied to a TSK gel DEAE-5PW column. IL-6 was eluted with a linear gradient of 0−150 mM NaCl in 5 mM Tris-HCl (pH 8.0). Positive fraction from a single peak was pooled, and an apparent 21 kDa single band was observed by SDS−polyacrylamide gel electrophoresis. From 1 L of culture medium, 10 mg of purified IL-6 was obtained. Site-directed mutagenesis was performed as described by Nishimura et al. (1991a, 1992), and all mutant IL-6's were obtained by the same purification procedures. There was no substantial difference between the WT and mutant IL-6's in the HPLC elution profile and final yield. For NMR studies in H_2O, purified IL-6's were dialyzed against 10 mM phosphate buffer (pH 7.7) containing 120 mM NaCl. The IL-6 solution was adjusted to pH 5.7 and concentrated to 0.4 mL by using an Amicon Centriprep 10 cartridge. D_2O was added to the sample to a final concentration of 10%, and a ca. 1 mM protein sample solution was prepared. For NMR studies in D_2O, purified IL-6 and IL-6 mutants were concentrated to 0.4 mL in 10 mM phosphate buffer (pH 7.7) containing 120 mM NaCl in D_2O.

NMR Measurements. Two-dimensional ^{1}H NMR spectra of the WT and mutant IL-6's were recorded at 500 MHz with a JEOL JNM-GSX 500 spectrometer with a spectral width of 7000 Hz. Nuclear Overhauser effect spectroscopy (NOESY) (Jeener et al., 1979) and homonuclear Hartmann−Hahn spectroscopy (HOHAHA) (Bax & Davis, 1985) were used in the phase-sensitive mode as described by States et al. (1982). 2K data points were used in the t_2 dimension, and 256 scans were acquired for 256 t_1 points with a relaxation delay of 1.0 s. NOESY and HOHAHA spectra were recorded with mixing times of 90 and 35 ms, respectively. Zero-filling was performed for the t_1 dimension, and the data matrix of 1K(F_2) × 512(F_1) was obtained. For both NOESY and HOHAHA spectra, a Gaussian function was applied for both the t_1 and t_2 dimensions.

^{1}H−^{15}N shift correlation spectra of IL-6 were recorded with spectral widths of 6000 Hz for ^{1}H and 600 Hz for ^{15}N on a Bruker AM 400 spectrometer equipped with a 5-W BFX-5 X-nuclear decoupler (Bodenhausen & Ruben, 1980). 1K data points were used in the t_2 dimension, and 256−448 scans were acquired for 32−128 t_1 points. F_1 quadrature was achieved by time-proportional phase incrementation (Marion & Wüthrich, 1983). The acquired data were zero-filled, and a Gaussian function was applied for both the t_1 and t_2 dimensions to yield a matrix 512(F_2) × 64−256(F_1) of the real data points. The solvent resonance was suppressed by combined use of selective, weak irradiation during

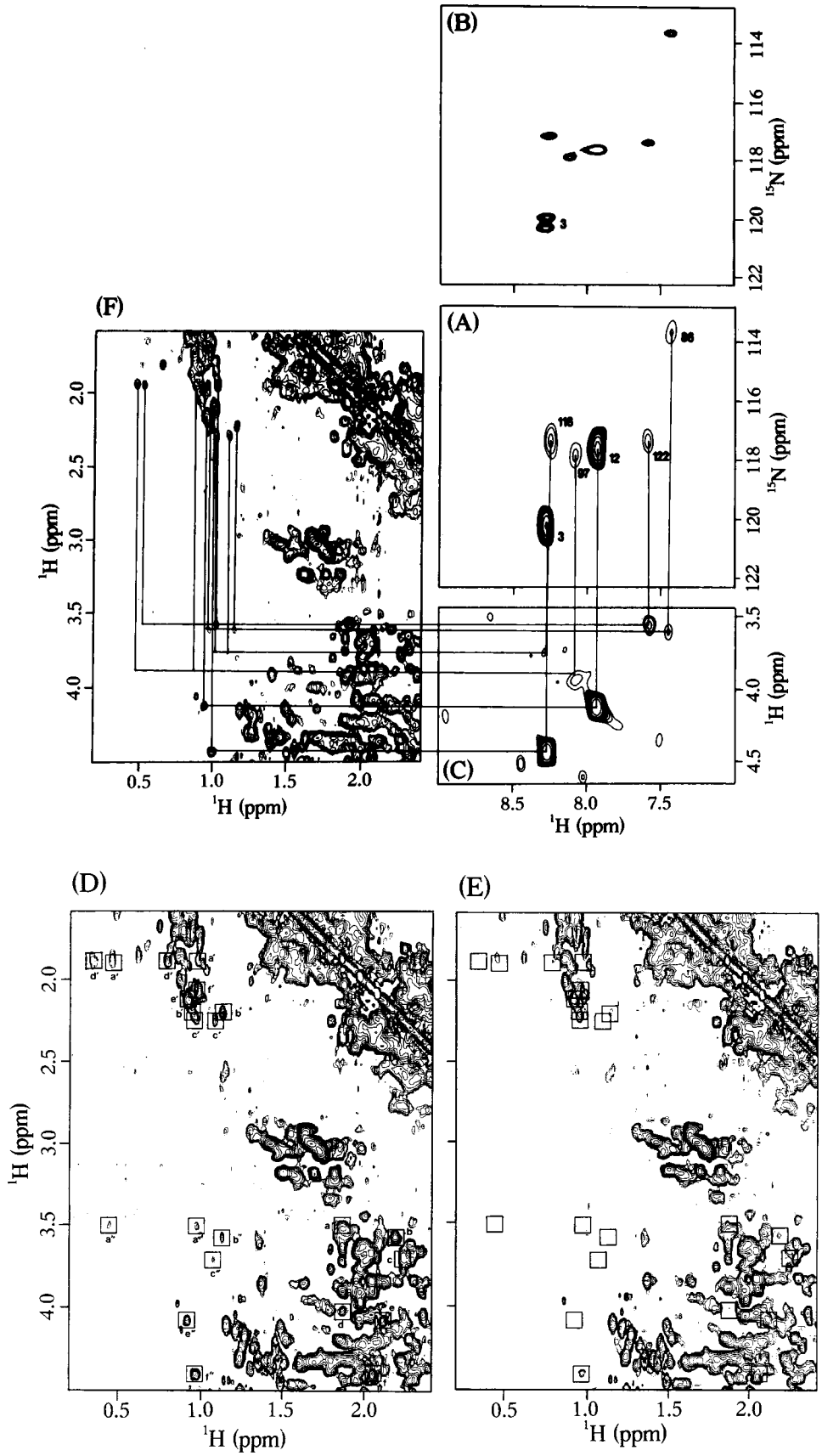

FIGURE 1: Signal assignments of amide, α-, *β*-, and *γ*-protons originating from six Val residues. ^{1}H−^{15}N shift correlation spectra of IL-6 labeled with [^{15}N]Val at pH 5.7 (A) and doubly labeled with [^{15}N]Val and [^{13}C]Pro at pH 5.7 (B). The signal assignments (residue numbers) of Val residues are indicated in (A). Amide and Cα-proton region of the ^{15}N-edited HOHAHA spectrum of IL-6 labeled with [^{15}N]Val at pH 5.7 (C). The mixing time was set to 40 ms. Aliphatic−aliphatic regions of 2D HOHAHA spectra of IL-6 at pH 7.7 (D) and pH 5.7 (F), and Val-d_8-substituted IL-6 at pH 7.7 (E). The mixing time was 35 ms. The assigned amide protons are connected to the α-, *β*-, and *γ*-protons by solid lines.

the preparation period of 1.2 s and a spin−lock purge pulse (Otting & Wüthrich, 1988).

^{15}N-edited HOHAHA and NOESY spectra of IL-6 were recorded with a spectral width of 6000 Hz for ^{1}H on a Bruker

AMX 500 spectrometer. 1K data points were used in the t_2 dimension, and 448 scans were acquired for 256 t_1 points. Mixing times were set to 40 ms for ^{15}N-edited HOHAHA and 80 ms for ^{15}N-edited NOESY. F_1 quadrature was achieved by time-proportional phase incrementation. The acquired data were zero-filled, and a Gaussian function was applied for both the t_1 and t_2 dimensions to yield a matrix 512(F_2) × 512(F_1) of the real data points. All NMR spectra were recorded at sample temperature of 30 °C.

RESULTS AND DISCUSSION

Site-Specific Assignments of the Side Chain Proton Resonances of Val, Ile, Leu, Phe, Tyr, His, and Trp Residues. To monitor the structural changes in human IL-6 induced by site-directed mutagenesis and to characterize the folding topology of human IL-6, spectral assignments were made for some of the resonances that originate from hydrophobic residues by using specific double-labeling and site-specific mutagenesis strategies (Campbell-Burk et al., 1989). For the assignment of the side chain protons of Val residues, [^{15}N]Val was incorporated into IL-6. Site-specific assignments for the amide proton resonances of Val residues were performed by a double-labeling method (Kainosho & Tsuji, 1982; Takahashi et al., 1991). The assigned amide protons were connected to the α-, β-, and γ-protons by measuring HOHAHA spectra.

IL-6 contains six Val residues. Figure 1A shows a ^{1}H−^{15}N shift correlation spectrum of [^{15}N]Val-labeled IL-6 at pH 5.7, in which six cross-peaks can be separately observed. The ^{1}H−^{15}N shift correlation spectrum of IL-6 that is doubly labeled with [1-^{13}C]Pro and [^{15}N]Val clearly shows that cross-peak "3" is due to Val3 (Figure 1B). In a similar way, four other Val signals were assigned to Val86, Val97, Val116, and Val122 by using double-labeled [^{15}N]Val analogs with [^{13}C]Leu, [^{13}C]Glu, [^{13}C]Ala, or [^{13}C]Lys (data not shown). The remaining signal was assigned to Val12. The results of the spectral assignments are indicated in Figure 1A.

The assigned amide proton resonances were connected to the corresponding Cα-proton resonances on the basis of the ^{15}N-edited HOHAHA spectrum at pH 5.7 (Figure 1C). All NH_i−$C\alpha H_i$ cross-peaks of the Val residues are observable in this spectrum. The chemical shifts of the Cγ-methyl proton resonances originating from the Val residues were determined by observing the HOHAHA transfer from an assigned Cα-proton through a Cβ-proton to Cγ-methyl protons. Figure 1D,E shows the 2D HOHAHA spectra of IL-6 observed at pH 7.7 that contain protonated and perdeuterated valines, respectively. No cross-peaks originating from the six Val residues are observed for Val-d_8-labeled IL-6 (Figure 1E). The connectivities of $C\alpha H_i$−$C\beta H_i$ (a−f), $C\beta H_i$−$C\gamma H_i$ (a′−f′), and $C\alpha H_i$−$C\gamma H_i$ (a″−f″) originating from six Val residues were achieved in Figure 1D. After the assignment of each resonance of Val residues in the HOHAHA spectrum at pH 7.7 (Figure 1D) to that at pH 5.7 (Figure 1F), the assigned Cα-proton resonances (Figure 1C) were connected to the corresponding Cγ-proton resonances on the basis of the 2D HOHAHA spectrum (Figure 1F).

In a similar way, the amide proton resonances for nine Ile residues and γCH_3 protons of Ile37, Ile137, and Ile167 were assigned (data not shown). It was not possible to unambiguously assign the resonances of the side chain protons originating from the six remaining Ile residues. This is because the spin systems for these Ile residues are not separately observable.

The spectral assignments for seven Phe residues were made in the same way as the Val residues (data not shown). Since Phe95, Phe126, and Phe174 are preceded by Glx in the amino acid sequence, it is not possible to assign the resonances by the double-labeling method. The ^{1}H−^{15}N cross-peaks of Phe95 and Phe126 were assigned by NOE cross-peak correlations between NH_i−NH_{i+1} protons in ^{15}N-edited NOESY spectra. The assigned amide protons were connected to α- and 2′,6′-protons by the combined use of ^{15}N-edited HOHAHA and ^{13}C-edited NOESY spectra (Odaka et al., 1992). The spin systems of the aromatic ring protons were finally confirmed by the measurement of a HOHAHA spectrum.

The resonances of the aromatic protons originating from two His, three Tyr, and one Trp residues were assigned and reported previously (Nishimura et al., 1990). The ^{1}H−^{15}N cross-peaks originating from His and Tyr residues were assigned by the double-labeling method (data not shown). Site-directed mutagenesis has been used for the NMR signal assignments of proteins (Schlichting et al., 1990; McManus & Riechmann, 1991; Penington & Rule, 1992). The side chain proton resonances of Leu152, Leu168, and Leu175 among 23 Leu residues were assigned by making use of the amino acid substitution of each of the Leu residues with Val (data not shown). This is because it is difficult to connect the assigned amide proton signals originating from Leu residues to the δ-methyl proton signals.

The results of the resonance assignments of Val, Ile, Leu, Phe, Tyr, His, and Trp residues are summarized in Table 1. Chemical shifts of amide protons are at pH 5.7, while those of the other protons are at pH 7.7. More cross-peaks were observed in HOHAHA and NOESY spectra at pH 7.7 than at pH 5.7, probably because IL-6 aggregates more easily at pH 5.7 than at pH 7.7. The HOHAHA and NOESY spectra of IL-6 were analyzed at pH 7.7, whereas ^{1}H−^{15}N shift correlation spectra of IL-6 were measured at pH 5.7 for the site-specific assignments of amide proton resonances by the double-labeling method. The ^{1}H−^{15}N cross-peak from Phe171 was not observed at pH 5.7, but was at pH 5.0.

NOE Network of Human IL-6. On the basis of the crystal structure of porcine growth hormone (Abdel-Meguid et al., 1987), Bazan has made a structure prediction for human IL-6 (Bazan, 1990, 1991). In the Bazan model, four helix elements exist as an up−up−down−down four-helix bundle comprising Pro19−Thr44 (helix A), Glu81−Gln103 (helix B), Glu111−Asp135 (helix C), and Asp161−Met185 (helix D). On the basis of the spectral assignments made for the Val, Ile, Leu, Phe, Tyr, His, and Trp residues, we analyzed the NOESY data of IL-6 to determine the spatial relationship between some of the residue pairs in the protein molecule. Although severe overlapping of NOE cross peaks was observed, particularly in the aliphatic−aliphatic region, it was possible to observe some of the NOE cross-peaks in the aromatic−aromatic, aromatic−aliphatic, and aliphatic−aliphatic regions. The NOE network observed in the WT IL-6 is shown in Figure 2, where the location of the helix elements predicted by Bazan (1991) is indicated. An NOE cross-peak for Ile30 and Leu175 is observed between the amide and side chain protons, whereas that for Phe171 and Phe174 exists between the α- and aromatic protons. Other NOE cross-peaks are observed between side chain protons.

Table 1: ^{1}H, ^{13}C, and ^{15}N Chemical Shifts of Val, Ile, Leu, Phe, Tyr, His, and Trp Residues at pH 5.7 or 7.7, 30 °C

	amide (pH 5.7)		others (pH 7.7)			
	$^{1}H^{a}$	$^{15}N^{b}$	α	Cα^{b}	β	γCH and others
Val3	8.28	120.1	4.40		2.04	γCH 0.97
Val12	7.94	117.6	4.07		2.10	γCH 0.92
His16	8.44	116.1				δCH 6.94; ϵCH 7.71
Ile26	7.91	118.8				
Ile30	8.40	115.9				
Tyr32	8.15	117.6				δCH 7.12; ϵCH 6.79
Ile33	8.08	119.6				
Ile37	8.78	118.7	3.57		1.86	γCH 0.86
Phe75	8.58	119.6	5.10	51.9		δCH 7.20; ϵCH, ζCH 7.08
Phe79	7.39	119.9	4.21	57.5		δCH 7.10; ϵCH 7.24; ζCH 7.17
Val86	7.42	113.6	3.58		2.18	γCH 0.94, 1.14
Ile88	8.91	118.3				
Ile89	8.45	115.2				
Phe95	8.29	113.5	4.41	60.8		δCH 6.93; ϵCH 6.84; ζCH 7.09
Val97	8.12	118.0	4.02		1.86	γCH 0.32, 0.78
Tyr98	6.99	117.8				δCH 6.88; ϵCH 6.52
Tyr101	7.84	118.6				δCH 6.93; ϵCH 6.64
Phe106	7.72	115.8	4.62	55.7		δCH 7.34; ϵCH, ζCH 7.00
Val116	8.26	117.2	3.72		2.22	γCH 0.97, 1.08
Val122	7.58	117.4	3.51		1.87	γCH 0.44, 0.98
Ile124	8.33	116.1				
Phe126	8.37	116.2	4.49	56.9		δCH 7.09; ϵCH, ζCH 7.22
Ile137	7.56	117.0	3.98		1.98	γCH 0.87
Leu152						γCH 1.42; δCH 0.72, 0.85
Trp158						ϵCH, ζCH 7.59, 7.47; ζCH, ηCH 7.21, 7.13
His165	7.86	117.0				δCH 6.89; ϵCH 7.68
Ile167	8.73	118.7	3.42		2.00	γCH 0.89
Leu168						γCH 1.22; δCH 0.04, 0.63
Phe171			4.04	56.5		δCH 6.08; ϵCH 6.78; ζCH 7.56
Phe174	8.99	122.4	4.29	60.6		δCH 7.10; ϵCH 7.34; ζCH 7.71
Leu175						γCH 1.69; δCH 0.23, 0.75

^{a} ^{1}H chemical shifts are expressed in ppm relative to DSS. ^{b} ^{13}C and ^{15}N chemical shifts are relative to TMS and formamide, respectively.

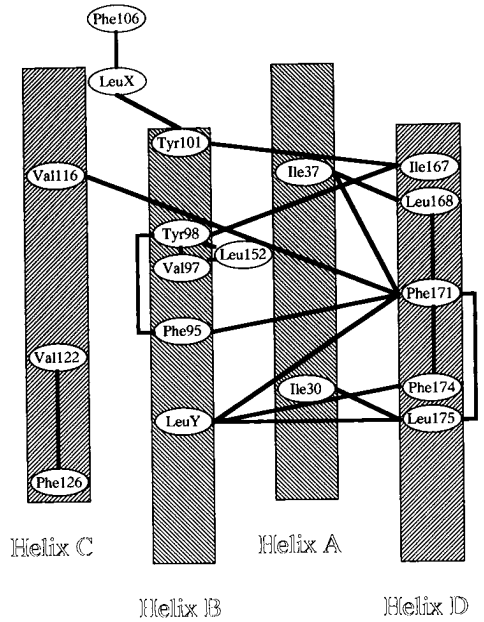

FIGURE 2: NOE network of human IL-6. NOE cross-peaks were observed between amino acid residue pairs connected by solid lines. The NOEs are compatible with the predicted up−up−down−down helix topology.

The NOEs obtained are quite consistent with the predicted up−up−down−down helix topology: (1) observation of the NOE cross-peaks for two residue pairs Ile30−Leu175 and Ile37−Leu168 indicates that helix A is antiparallel to helix D, and (2) NOE cross-peaks for the two residue pairs Phe95−Phe171 and Tyr101−Ile167 show that helix B is antiparallel to helix D. Other NOEs are also consistent with the Bazan model.

^{1}H Chemical Shift Difference between the WT IL-6 and Six IL-6 Mutants. Previous site-directed mutagenesis studies of IL-6 have shown that the amino acid residues in the C-terminal region play an important role in the gp80 receptor binding. The gp80 receptor-binding activities of the WT and six IL-6 mutants have been reported previously (Nishimura et al., 1991a, 1992). The most pronounced effect on the activity was observed in the case of the IL-6 mutant substituted at Leu175 by the Val residue (activity 8% that of WT IL-6). This mutant hereafter will be designated as L175V. Similar notation will also be used for the other mutants. This result shows that Leu175 plays the most important role in the receptor binding of IL-6. Effects of mutation on the receptor-binding activity observed for L168V (activity 20% that of WT IL-6) and L182V (17%) are greater than those for L152V (80%), L159V (96%), and L166V (61%).

To examine the structural changes induced by the amino acid substitutions, the 2D HOHAHA spectra of the WT and six mutated IL-6's were compared. The chemical shift differences observed for the WT and mutant IL-6's were used for probing induced structural changes. Figure 3 shows the aromatic−aromatic region of the 2D HOHAHA spectrum of the WT IL-6. The spin systems of 13 aromatic residues are indicated. Since the 2D HOHAHA spectra of the six mutants are largely similar to that of the WT IL-6 (data not shown), the proton resonances in the spectra of the mutants were assigned in comparison to those in the spectrum of the WT IL-6. Chemical shift differences observed between the WT IL-6 and each one of the six IL-6 mutants are summarized in Figure 4A−F. Chemical shift and NOE data are discussed on the basis of the location of four helix

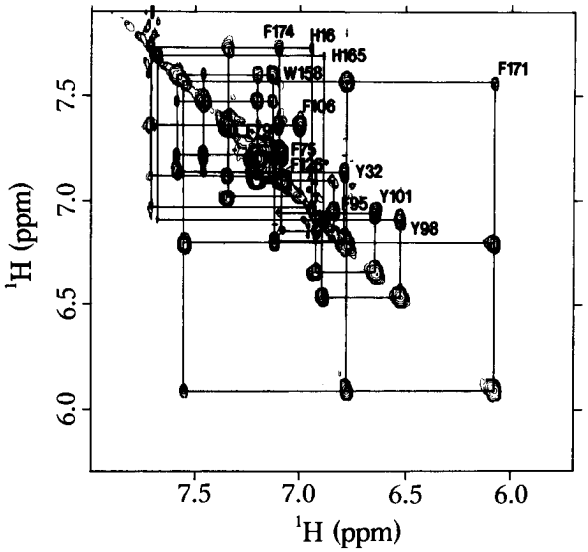

FIGURE 3: Aromatic−aromatic region of the 2D HOHAHA spectrum of WT IL-6 at pH 7.7. The mixing time was 35 ms. The signal assignments of aromatic protons are indicated.

elements and an up−up−down−down helix topology of the predicted structure of IL-6 (Bazan, 1991).

No difference in chemical shifts is observed between L182V and WT IL-6 (Figure 4F), indicating that no structural change was induced by the amino acid substitution. It is probable that Leu182 is located on the surface of the protein. In the case of L182V, a significant decrease in receptor-binding activity was observed compared with WT IL-6 (Nishimura et al., 1992). We suggest that the side chain of Leu182 is directly involved in receptor binding on the protein surface. No significant spectral change was observed in L159V and L166V (Figure 4B,C).

Substitution of either Leu168 or Leu175 with Val caused significant changes in the spectra (Figure 4D,E). Major changes are shifts in the resonances of Phe95, Leu168, Phe171, Phe174, and Leu175, which exist in the regions of helices B and D. In the case of L175V, differences in the chemical shifts of Tyr32, Val116, and Val122 are also observed. It is possible that the structural changes indicated by the chemical shift changes observed in L168V and L175V are related to the decrease in those receptor-binding activities (Nishimura et al., 1992). Substitution of Leu152 with Val induced large spectral changes (Figure 4A). The differences in the chemical shifts of resonances originating from Ile37, Phe95, Val97, Tyr98, Tyr101, Phe106, Ile137, Leu152, Trp158, Leu168, Phe171, Phe174, and Leu175 are observed. Since Leu152, Leu168, and Leu175 probably play a role in forming hydrophobic packing (Figure 2), the mutations of their residues might induce the significant structural changes in the IL-6 molecule.

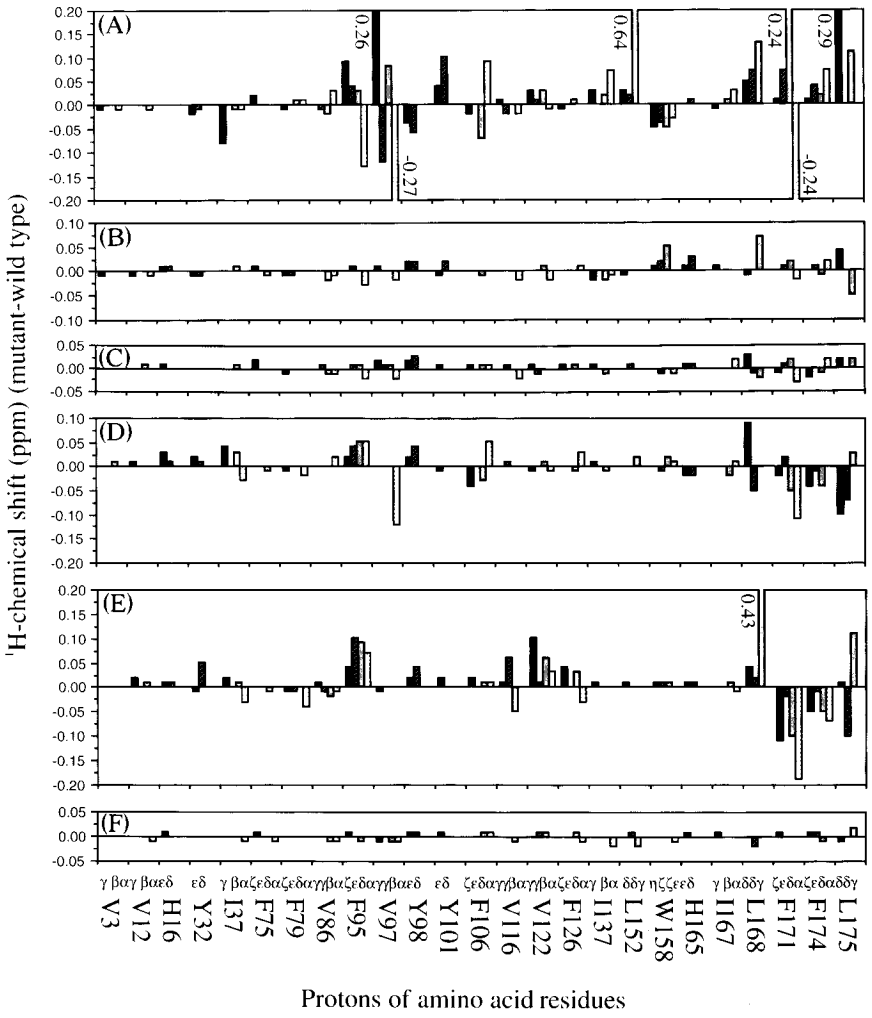

FIGURE 4: Changes in chemical shifts of proton resonances originating from assigned residues in IL-6 induced by Leu152 (A), Leu159 (B), Leu166 (C), Leu168 (D), Leu175 (E), and Leu182 (F) substitutions with Val. In the case of chemical shift changes of more than 0.2 ppm compared with that of WT IL-6, values of chemical shift change are shown next to the bars.

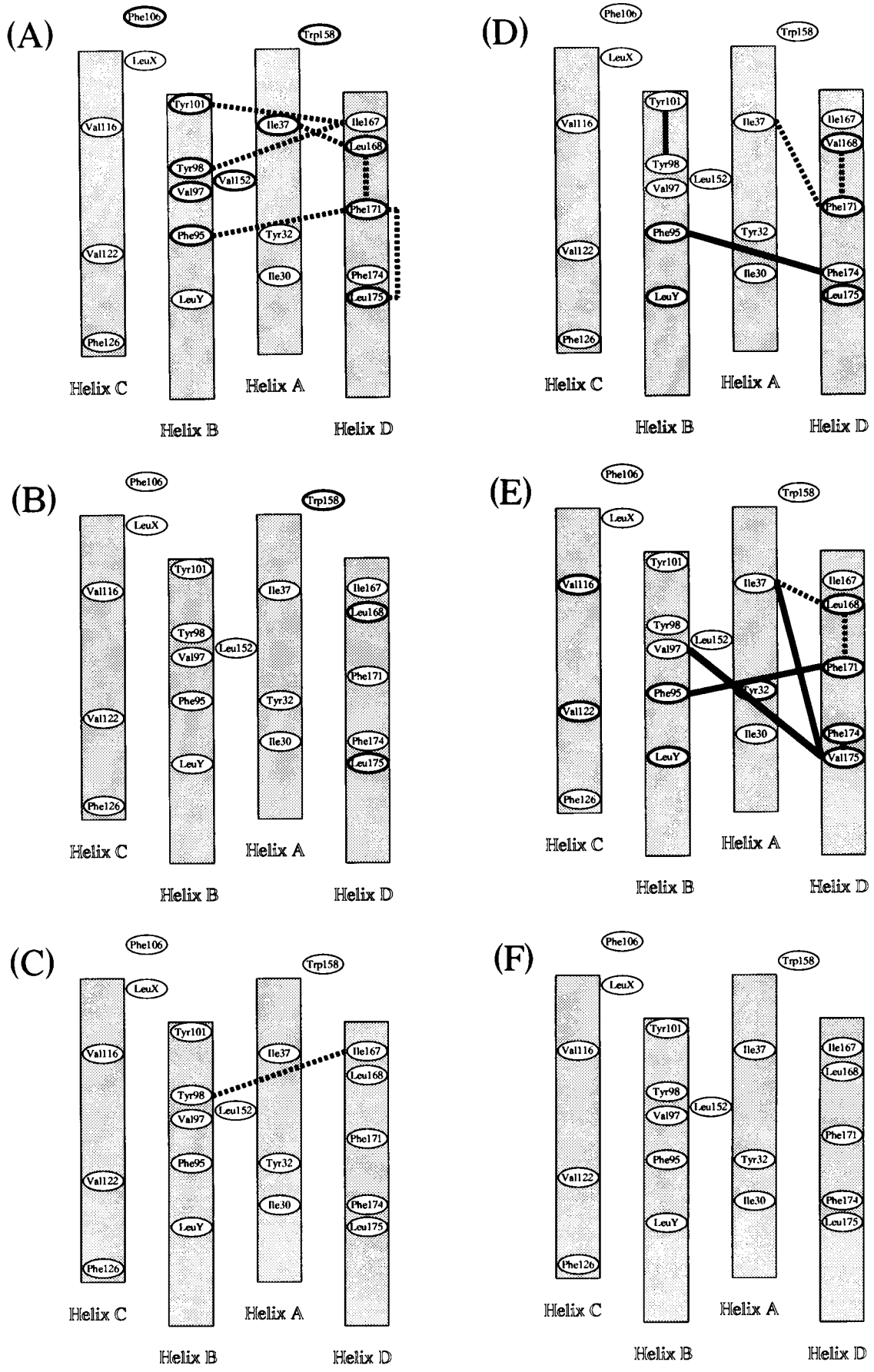

FIGURE 5: Comparison of NOE networks of L152V (A), L159V (B), L166V (C), L168V (D), L175V (E), and L182V (F) with that of WT IL-6. Only the decrease and increase in intensity of NOEs compared with that of WT IL-6 are expressed in dashed and solid lines, respectively. The residues in which at least a side chain proton resonance indicates a chemical shift change greater than 0.05 ppm are encircled.

Table 2: Hydrophobic Amino Acid Residues Conserved in the Sequence Alignment between Human IL-6 and G-CSF

	human IL-6	human G-CSF
helix A	Ile30, Ile33, Ile37	Val21, Ile24, Gly28
helix B	Leu92, Phe95, Val97, Tyr98, Leu99, Tyr101	Leu82, Tyr85, Gly87, Leu88, Leu89, Ala91
helix C	Val116, Thr120, Leu123	Leu106, Val110, Phe113
loop C−D	Leu152	Phe140
helix D	Ile167, Leu168, Phe171, Phe174, Leu175	Val153, Ala154, Leu157, Phe160, Leu161

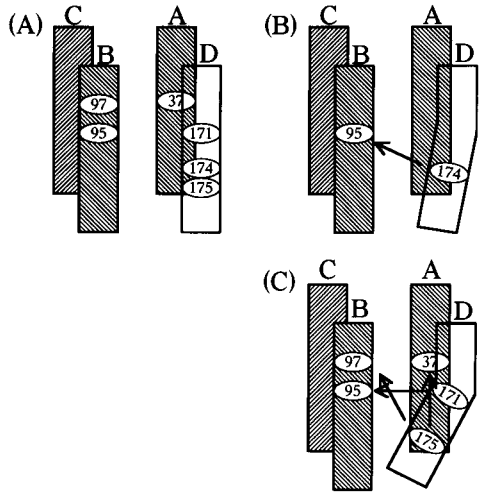

FIGURE 6: Schematic diagrams of four-helix bundle structures of WT IL-6 (A), L168V (B), and L175V (C). A−D represent the four helices. Arrows represent paired residues between which either an increase in NOE intensity or the appearance of new NOE cross-peaks induced by substitution of Leu168 or Leu175 with Val was observed.

Differences in NOE Networks between the WT and Six IL-6 Mutants. On the basis of spectral assignments of the six IL-6 mutants, NOESY spectra of the mutants were analyzed to determine spatial relations between some proton pairs. Figure 5A−F summarizes the changes in NOE networks induced by the Leu→Val substitutions. The residues, in which at least one of the side chain proton resonances gives a chemical shift change greater than 0.05 ppm, are also shown in Figure 5A−F.

NOE networks of L159V (Figure 5B) and L182V (Figure 5F) are virtually identical to that of WT IL-6. These results indicate that neither mutation induced a significant structural change in IL-6. In the case of L166V, no difference but the decrease in intensity of the NOE between Tyr98 and Ile167 is observed (Figure 5C) compared with WT IL-6.

In the case of L175V, a significant decrease in intensity was observed for NOEs between two pairs of residues, Ile37 and Leu168 and Leu168 and Phe171. By contrast, new cross-peaks of NOEs became observable between three pairs, Val97 and Val175, Ile37 and Val175, and Phe174 and Val175, in addition to the NOEs observed in the case of WT IL-6. Moreover, a significant increase in intensity was observed for the NOE between Phe95 and Phe171 (Figure 5E). It is possible that helix D bent toward helix B to maintain the hydrophobic packing in the region of mutated Val175. This is because Phe171 is in closer proximity to Phe95 in L175V than in WT IL-6 and because Ile37 and Val97, which are shown in the NOE network to be located near Leu168 rather than Leu175 in WT IL-6, come to be near Val175 in L175V. This is also consistent with the result that the values of chemical shifts of α-proton resonances of Phe171 and Phe174 of WT IL-6 (4.04 and 4.29 ppm) and L175V (3.85 and 4.22 ppm), respectively (Table 1 and Figure 4E), indicate that even after L175V mutation the secondary structure of the region in which these two residues exist remains an α-helix on the basis of the chemical shift index (Wishart et al., 1992). It was reported that both helices A and D in murine LIF and helix D in human G-CSF exhibit pronounced kinks (Robinson et al., 1994; Hill et al., 1993). This suggests that the long and straight helix has to be bent in order to maximize the region of a closely packed and solvent-inaccessible core in the LIF and G-CSF molecules. Although it is not clear whether helix D in WT IL-6 exhibits a pronounced kink, we suggest that a sharper kink in helix D than that in WT IL-6 occurs in the case of L175V (Figure 6C). It is possible that the kink in helix D in L175V is related to the decrease in receptor-binding activity (Nishimura et al., 1992). Ser170 is the most probable candidate for the breaker of the α-helical hydrogen bond in helix D, because the polar side chain of the Ser residue is capable of hydrogen bond formation. Chemical shift changes of the resonances of Tyr32, Val116, and Val122 and upfield shifts of the resonances of Phe171, Phe174, and Val175 observed for L175V (Figures 4E and 5E) might be due to the bending of helix D toward helix B. In the case of L168V, it is probable that helix D is more closely attached to helix B because a new NOE cross-peak became observable between Phe95 and Phe174 compared to the case of WT IL-6 (Figure 5D). On the basis of this NOE and upfield shifts of resonances of Phe171, Phe174, and Leu175 observed in L168V (Figure 4D), it may be possible that a less sharp kink in helix D occurs in L168V than that observed in L175V (Figure 6B).

In the case of L152V, a significant decrease in NOE intensity between six residue pairs is observed (Figure 5A). This indicates that the hydrophobic packing formed by the residues existing in helices A, B, and D was partially disrupted. However, no difference in receptor-binding activity between WT IL-6 and L152V was observed. It is not clear why no decrease in receptor-binding activity was observed in L152V even though such drastic changes in chemical shift and NOE network occurred. It is possible that the three-dimensional structure essential for the receptor-binding activity was conserved even after the mutation.

Comparison of Folding Topology of Human IL-6 with That of Human G-CSF. Human IL-6 shows a significant degree of sequence homology to human G-CSF, with 17% and 31% conservation of sequence identity and similarity, respectively (Bazan, 1991). The similarity of the hydrophobicity pattern in the amino acid sequences is observed between IL-6 and G-CSF (Savino et al., 1993). To compare the folding topology of IL-6 with that of human G-CSF, the NOEs of IL-6 were closely examined (Figure 2). The network of interhelical NOEs is composed of the hydrophobic residues, i.e., Ile30, Ile37, Leu*Y* (tentatively assigned to Leu92), Phe95, Tyr98, Tyr101, Val116, Ile167, Leu168, Phe171, Phe174, and Leu175. It is possible that these residues are involved in the hydrophobic packing of the four-helix bundle. NOE cross-peaks were observed between the aromatic ring of Phe171 and Ile37, Phe95, and Val116 that exist in the other

three helices. We therefore suggest that the aromatic ring of Phe171 points toward the hydrophobic helix bundle core. Table 2 shows that the 18 hydrophobic amino acid residues in IL-6 are well conserved in the corresponding region in the amino acid sequence of human G-CSF. The three-dimensional structure of human G-CSF determined by X-ray crystallography (Hill et al., 1993) indicates that these residues conserved in G-CSF are also involved in the hydrophobic packing of the four-helix bundle in a manner similar to that observed in IL-6. We therefore suggest that IL-6 and G-CSF are significantly similar to each other not only in amino acid sequence but also in folding topology.

REFERENCES

Abdel-Meguid, S. S., Shieh, H.-S., Smith, W. W., Dayringer, H. E., Violand, B. N., & Bentle, L. A. (1987) *Proc. Natl. Acad. Sci. U.S.A 84*, 6434−6437.

Asagoe, Y., Yasukawa, K., Saito, T., Maruo, N., Miyata, K., Kono, T., Miyake, T., Kato, T., Kadidani, H., & Mitani, M. (1988) *Biotechnology 6*, 806−809.

Bax, A., & Davis, D. G. (1985) *J. Magn. Reson. 65*, 355−366.

Bazan, J. F. (1990) *Immunol. Today 11*, 350−354.

Bazan, J. F. (1991) *Neuron 7*, 197−208.

Bodenhausen, G., & Ruben, D. J. (1980) *Chem. Phys. Lett. 69*, 185−189.

Brakenhoff, J. P. J., de Hon, F. D., Fontaine, V., ten Boekel, E., Schooltink, H., Rose-John, S., Heinrich, P., Content, J., & Aarden, L. A. (1994) *J. Biol. Chem. 269*, 86−93.

Campbell-Burk, S., Papastavros, M. Z., McCormick, F., & Redfield, A. G. (1989) *Proc. Natl. Acad. Sci. U.S.A. 86*, 817−820.

de Vos, A. M., Ultsch, M., & Kossiakoff, A. A. (1992) *Science 255*, 306−312.

Ehlers, M., Grötzinger, J., de Hon, F. D., Müllberg, J., Brakenhoff, J. P. J., Liu, J., Wollmer, A., & Rose-John, S. (1994) *J. Immunol. 153*, 1744−1753.

Ehlers, M., de Hon, F. D., Bos, H. K., Horsten, U., Kurapkat, G., van De Leur, H. S., Grötzinger, J., Wollmer, A., Brakenhoff, J. P. J., & Rosen-John, S. (1995) *J. Biol. Chem. 270*, 8158−8163.

Fontaine, V., Ooms, J., & Content, J. (1994) *Eur. J. Immunol. 24*, 1041−1045.

Hill, C. P., Osslund, T. D., & Eisenberg, D. (1993) *Proc. Natl. Acad. Sci. U.S.A. 90*, 5167−5171.

Jeener, J., Meier, B. H., Bachmann, P., & Ernst, R. R. (1979) *J. Chem. Phys. 71*, 4546−4553.

Kainosho, M., & Tsuji, T. (1982) *Biochemistry 21*, 6273−6279.

Kishimoto, T., & Hirano, T. (1988) *Annu. Rev. Immunol. 6*, 485−512.

Kishimoto, T., Akira, S., & Taga, T. (1992) *Science 258*, 593−597.

Krüttgen, A., Rose-John, S., Dufhues, G., Bender, S., Lütticken, C., Freyer, P., & Heinrich, P. C. (1990) *FEBS Lett. 273*, 95−98.

Leebeek, F. W. G., Kariya, K., Schwabe, M., & Fowlkes, D. M. (1992) *J. Biol. Chem. 267*, 14832−14838.

Marion, D., & Wüthrich, K. (1983) *Biochem. Biophys. Res. Commun. 113*, 967−974.

McManus, S., & Riechmann, L. (1991) *Biochemistry 30*, 5851−5857.

Morton, C. J., Bai, H., Zhang, J.-G., Hammacher, A., Norton, R. S., Simpson, R. J., & Mabbutt, B. C. (1995) *Biochim. Biophys. Acta 1249*, 189−203.

Nishimura, C., Hanzawa, H., Itoh, S., Yasukawa, K., Shimada, I., Kishimoto, T., & Arata, Y. (1990) *Biochim. Biophys. Acta 1041*, 243−249.

Nishimura, C., Futatsugi, K., Yasukawa, K., Kishimoto, T., & Arata, Y. (1991a) *FEBS Lett. 281*, 167−169.

Nishimura, C., Ekida, T., Masuda, S., Futatsugi, K., Itoh, S., Yasukawa, K., Kishimoto, T., & Arata, Y. (1991b) *Eur. J. Biochem. 196*, 377−384.

Nishimura, C., Ekida, T., Nomura, K., Sakamoto, K., Suzuki, H., Yasukawa, K., Kishimoto, T., & Arata, Y. (1992) *FEBS Lett. 311*, 271−275.

Odaka, A., Kim, J. I., Takahashi, H., Shimada, I., & Arata, Y. (1992) *Biochemistry 31*, 10686−10691.

Otting, G., & Wüthrich, K. (1988) *J. Magn. Reson. 76*, 569−574.

Paonessa, G., Graziani, R., De Serio, A., Savino, R., Ciapponi, L., Lahm, A., Salvati, A. L., Toniatti, C., & Ciliberto, G. (1995) *EMBO J. 14*, 1942−1951.

Penington, C. J., & Rule, G. S. (1992) *Biochemistry 31*, 2912−2920.

Proudfoot, A. E., Brown, S. C., Bernard, A. R., Bonnefoy, J. Y., & Kawashima, E. H. (1993) *J. Protein Chem. 12*, 489−497.

Robinson, R. C., Grey, L. M., Staunton, D., Vankelecom, H., Vernallis, A. B., Moreau, J.-F., Stuart, D. I., Heath, J. K., & Jones, E. Y. (1994) *Cell 77*, 1101−1116.

Savino, R., Lahm, A., Giorgio, M., Cabibbo, A., Tramontano, A., & Ciliberto, G. (1993) *Proc. Natl. Acad. Sci. U.S.A. 90*, 4067−4071.

Savino, R., Lahm, A., Salvati, A. L., Ciapponi, L., Sporeno, E., Altamura, S., Paonessa, G., Toniatti, C., & Ciliberto, G. (1994a) *EMBO J. 13*, 1357−1367.

Savino, R., Ciapponi, L., Lahm, A., Demartis, A., Cabibbo, A., Toniatti, C., Delmastro, P., Altamura, S., & Ciliberto, G. (1994b) *EMBO J. 13*, 5863−5870.

Schlichting, I., John, J., Frech, M., Chardin, P., Wittinghofer, A., Zimmermann, H., & Rosch, P. (1990) *Biochemistry 29*, 504−511.

Senda, T., Shimazu, T., Matsuda, S., Kawano, G., Shimizu, H., Nakamura, K. T., & Mitsui, Y. (1992) *EMBO J. 11*, 3193−3201.

Sprang, S. R., & Bazan, J. F. (1993) *Curr. Biol. 3*, 815−827.

States, D. J., Haberkorn, R. A., & Ruben, D. J. (1982) *J. Magn. Reson. 48*, 286−292.

Taga, T., Hibi, M., Hirata, Y., Yamasaki, K., Yasukawa, K., Matsuda, T., Hirano, T., & Kishimoto, T. (1989) *Cell 58*, 573−581.

Takahashi, H., Odaka, A., Kawaminami, S., Matsunaga, C., Kato, K., Shimada, I., & Arata, Y. (1991) *Biochemistry 30*, 6611−6619.

Wishart, D. S., Sykes, B. D., & Richards, F. M. (1992) *Biochemistry 31*, 1647−1651.

BI951949E